Pathogenesis and treatment of autosomal-dominant nephrogenic diabetes insipidus caused by an aquaporin 2 mutation

Eisei Sohara*, Tatemitsu Rai*, Sung-Sen Yang*, Keiko Uchida†, Kosaku Nitta†, Shigeru Horita†, Mayuko Ohno†, Akihiro Harada‡, Sei Sasaki*, and Shinichi Uchida*§

*Department of Nephrology, Graduate School of Medicine, Tokyo Medical and Dental University, 1-5-45 Yushima, Bunkyo, Tokyo 113-8519, Japan; †Department of Medicine, Kidney Center, Tokyo Women's Medical University, 8-1 Kawadacho, Shinjuku, Tokyo 162-8666, Japan; and ‡Laboratory of Molecular Traffic, Department of Molecular and Cellular Biology, Institute for Molecular and Cellular Regulation, Gunma University, 3-39-15 Shouwamachi, Maebashi, Gunma 371-8512, Japan

Edited by Maurice B. Burg, National Institutes of Health, Bethesda, MD, and approved July 28, 2006 (received for review March 22, 2006)

Frame-shift mutations within the C terminus of aquaporin 2 (AQP2) cause autosomal-dominant nephrogenic diabetes insipidus (AD-NDI). To identify the molecular mechanism(s) of this disease *in vivo* and to test possible therapeutic strategies, we generated a mutant AQP2 (763–772 del) knockin mouse. Heterozygous knockin mice showed a severely impaired urine-concentrating ability. However, they were able to slightly increase urine osmolality after dehydration. This milder phenotype, when compared with autosomal-recessive NDI, is a feature of AD-NDI in humans, thus suggesting successful establishment of an AD-NDI mouse model. Immunofluorescence of collecting duct cells in the AD-NDI mouse revealed that the mutant AQP2 was missorted to the basolateral instead of apical plasma membrane. Furthermore, the mutant AQP2 formed a heterooligomer with wild-type AQP2 and showed a dominant-negative effect on the normal apical sorting of wild-type AQP2 even under dehydration. Using this knockin mouse, we tested several drugs for treatment of AD-NDI and found that rolipram, a phosphodiesterase 4 inhibitor, was able to increase urine osmolality. Phosphodiesterase inhibitors may thus be useful drugs for the treatment of AD-NDI. This animal model demonstrates that a mutant monomer gains a dominant-negative effect that reverses the normal polarized sorting of multimers.

knockin mouse | phosphodiesterase | sorting disorder

The aquaporin 2 (AQP2) water channel is a vasopressin-regulated water channel expressed in collecting duct epithelium (1). Vasopressin increases cAMP levels in collecting duct cells and induces a redistribution of AQP2 from intracellular vesicles to the apical membrane (2–4). This redistribution of AQP2 increases the water permeability of the collecting ducts and enables water reabsorption from hypotonic urine to the hypertonic medullary interstitium. Accordingly, mutations in the human AQP2 gene cause urine concentration defects, i.e., nephrogenic diabetes insipidus (NDI; ref. 5). There are two types of NDI caused by AQP2 mutations: autosomal-recessive and autosomal-dominant (AD; refs. 5 and 6).

Previously, our group identified three frameshift mutations in the C terminus of AQP2 in patients exhibiting AD-NDI (7); deletion of G at nucleotide position 721 (721 del G), deletion of 10 nucleotides starting from nucleotide position 763 (763–772 del), and deletion of seven nucleotides starting from nucleotide position 812 (812–818 del). All of these mutations cause shifts in the ORF and add 61 common residues to the C termini. We assayed the function of these mutants as water channels in *Xenopus* oocytes and found they did not increase water permeability because of a lack of plasma membrane expression (7). Further study in Madin–Darby canine kidney cells showed that mutant AQP2 was seen in the basolateral plasma membranes, whereas wild-type AQP2 was seen in the apical membranes (8). Although the overexpressed mutant showed dominant-negative effects over wild-type AQP2 in terms of intracellular localization, i.e., the mutant recruited the wild-type AQP2 from the apical to basolateral membranes, it remains unclear whether this is the true mechanism of the disease *in vivo*, because levels of expression of wild-type and mutant AQP2 could not be controlled in the cotransfection experiments.

To accurately assess the mechanism of diseases of dominant inheritance, expression of the wild-type and mutant proteins must be driven by the same promoter. Because AQPs are known to form tetramers, the molar ratio of wild-type and mutant proteins is particularly important for dominant-negative effects. In fact, we previously attempted to generate an AD-NDI mouse model using a transgenic strategy in which mutant expression was driven by the human AQP2 promoter. However, transgenic mice showed minimal phenotype because of small amounts of mutant AQP2 expression in the collecting ducts. Accordingly, to further investigate the pathogenesis and treatment, we attempted to generate a true disease model of AD-NDI using a knockin mouse strategy.

Results

Generation of Mutant AQP2 (763–772 del) Knockin Mice. As shown in Fig. 1 *A* and *B*, the construct for the mutant AQP2 (763–772 del) knockin mice was designed to express the chimeric mutant AQP2 protein whose C terminus was exchanged with that of the human AQP2 (763–772 del) mutant. To generate the knockin mouse, we used homologous recombination in ES cells to create a mutant allele (Fig. 1*A*). We crossed the chimeric mice from recombinant ES clones with C57BL/6 mice to produce mutant AQP2 (763–772 del, flox/+) mice. The generation of mutant AQP2 (flox/+) mice was verified by PCR (Fig. 1*C*). Additional Southern blot analysis was used to verify the results of PCR (Fig. 1*D*). To delete the neocassette from the *aqp2* gene, we crossed mutant AQP2 (flox/+) mice with Cre recombinase-expressing transgenic mice (9). The *cre*-mediated excision of the neocassette was verified by PCR, as shown in Fig. 1*E* (lane H neo−). The expression of wild-type and mutant AQP2 proteins was confirmed by immunoblotting (Fig. 1*F*). The abundance of wild-type AQP2 in the heterozygous knockin mouse appeared to be unchanged compared with that in the wild-type mouse. The relative expression of wild-type and mutant AQP2 protein in the heterozygous knockin mice was estimated by using anti-AQP2 antibody (Santa Cruz Biotechnology, Santa Cruz, CA), which recognizes both

Author contributions: S.S. and S.U. designed research; E.S., T.R., S.-S.Y., K.U., K.N., S.H., and M.O. performed research; and A.H. contributed new reagents/analytic tools.

The authors declare no conflict of interest.

This paper was submitted directly (Track II) to the PNAS office.

Abbreviations: AD, autosomal-dominant; NDI, nephrogenic diabetes insipidus; AQP2, aquaporin 2; PDE, phosphodiesterase; dDAVP, 1-deamino-8-D-arginine vasopressin.

§To whom correspondence should be addressed. E-mail: suchida.kid@tmd.ac.jp.

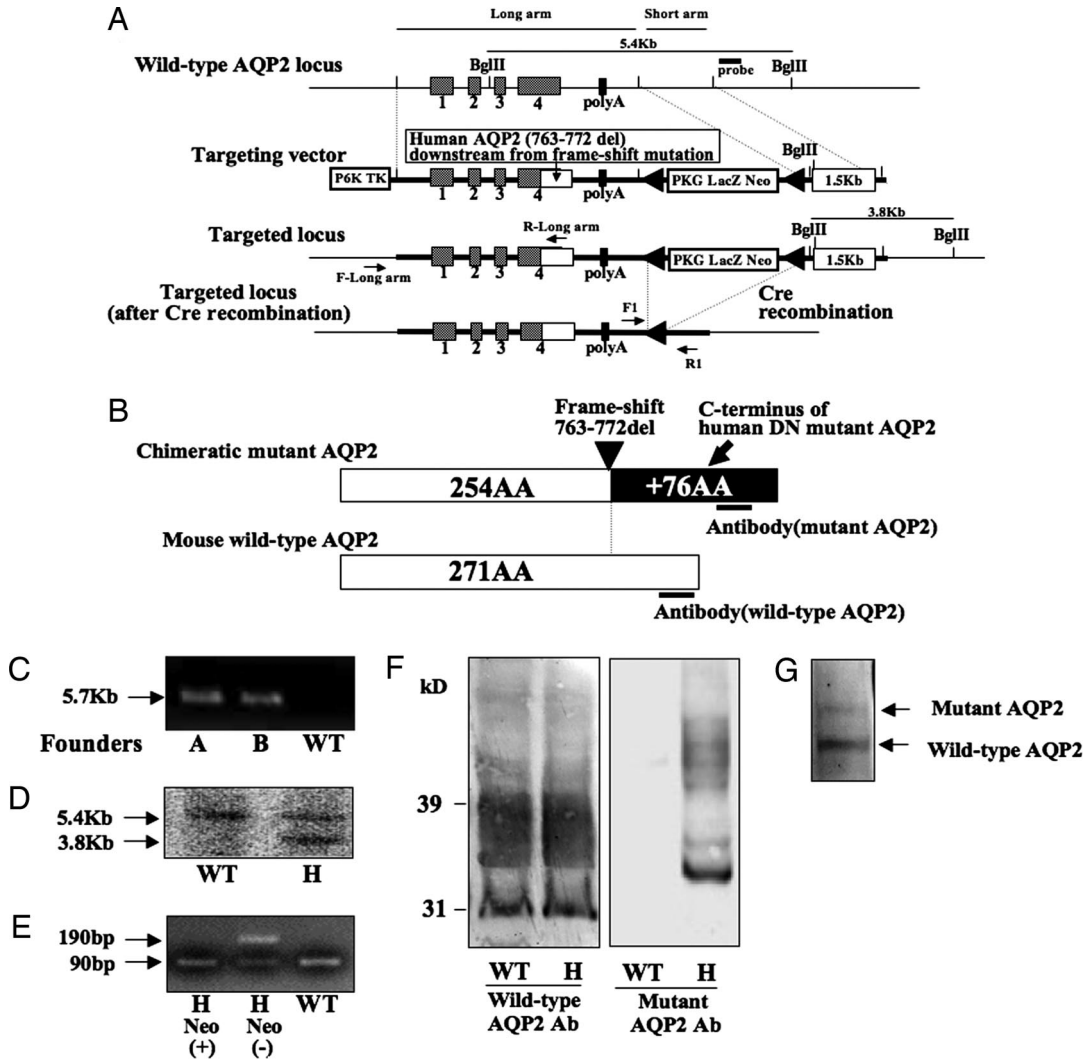

Fig. 1. Generation of mutant AQP2 (763–772 del) knockin mice. (*A*) Targeting strategy for generating mutant AQP2 (763–772 del) knockin mice. The diagram shows the wild-type AQP2 locus, the targeting construct, and the targeted locus before and after Cre recombination. The construct was designed to express a chimeric mutant AQP2 protein whose C terminus was exchanged with that of human mutant AQP2 (763–772 del). Two loxPs were inserted to flank the LacZ-Neo selective marker. The neocassette was deleted by mating the flox mice with CAG promoter Cre recombinase mice. (*B*) Structure of the chimeric mutant AQP2 protein expressed in the knockin mice. The C terminus of mouse wild-type AQP2 was exchanged with that of human mutant AQP2, which is thought to have a dominant-negative effect. Wild-type and mutant AQP2 antibodies were prepared to avoid cross-reactions. (*C*) Verification of homologous recombination by PCR of genomic DNA of the mice and amplification of the long arm of the construct using primer set F- and R-long arm was as shown in *A*. The 5.7-kb band is from the mutated allele. The primer set was designed not to amplify wild-type AQP2 gene. (*D*) Verification of homologous recombination by Southern blotting of BglII-digested genomic DNA derived from mouse tails. The 5.4-kb band is from the wild-type allele, and the 3.8-kb band is from the mutated allele. (*E*) Genotyping PCR after Cre recombination using a primer set flanking the remaining loxP site (F_1 and R_1). The 190-bp band represents the mutant allele containing the remaining loxP site, whereas the 90-bp band represents the wild-type allele. (*F*) Immunoblot of kidney homogenate probed with anti-wild-type AQP2 or mutant AQP2 antibody. Wild-type AQP2 (30-kDa band and higher glycosylated form) is expressed in both the wild-type and the heterozygous mutant AQP2 knockin mouse. Only the heterozygous knockin mouse exhibited expression of chimeric mutant AQP2 (34-kDa band and higher glycosylated form) in the kidney. H, heterozygous. (*G*) Immunoblot of deglycosylated proteins from papillae of heterozygous knockin mice probed with anti-AQP2 antibody, which recognizes the N-terminal portion of AQP2 (Santa Cruz Biotechnology). The relative amount of mutant AQP2 to wild-type AQP2 was estimated to be ≈30%.

proteins. Because the nonglycosylated mutant AQP2 band (≈34 kDa) was embedded in the smear band of glycosylated AQP2, we first treated the protein sample from the knockin mice with *N*-glycosidase F and then used it in the Western blotting analysis. As shown in Fig. 1*G*, the expression levels were not equal; the amount of mutant AQP2 was ≈30% of the wild-type AQP2 level.

Urinary-Concentrating Defects in Mutant AQP2 (763–772 del) Knockin Mice. As shown in Fig. 2*A*, under normal conditions, urine volume increased significantly in heterozygous AQP2 knockin mice when compared with wild-type mice (5.5 ± 1.8 vs. 0.85 ± 0.6 ml per day, respectively, $n = 4$, $P < 0.03$). Similarly, before and after a 24-hr water-deprivation period, urine osmolality was significantly reduced in heterozygous knockin mice, when compared with wild-type mice (240 ± 54 vs. 2470 ± 530 mOsm/kg H_2O, respectively, before water deprivation, $P < 0.001$; 1,120 ± 406 vs. 3,760 ± 579 mOsm/kg H_2O, respectively, after water deprivation, $P < 0.001$, $n = 4$; Fig. 2*B*). Furthermore, after dehydration, significantly greater weight loss was observed among heterozygous knockin than in wild-type mice (24.2 ± 2.4 vs. 13.9 ± 1.3%, respectively, $n = 4$, $P < 0.01$; Fig. 2*C*). Maximal urine osmolality after i.p. injection of 1-deamino-8-D-arginine vasopressin (dDAVP) was also significantly reduced in heterozygous knockin as compared with wild-type mice (644 ± 188 vs. 2,928 ± 436 mOsm/kg H_2O, respectively, $n =$

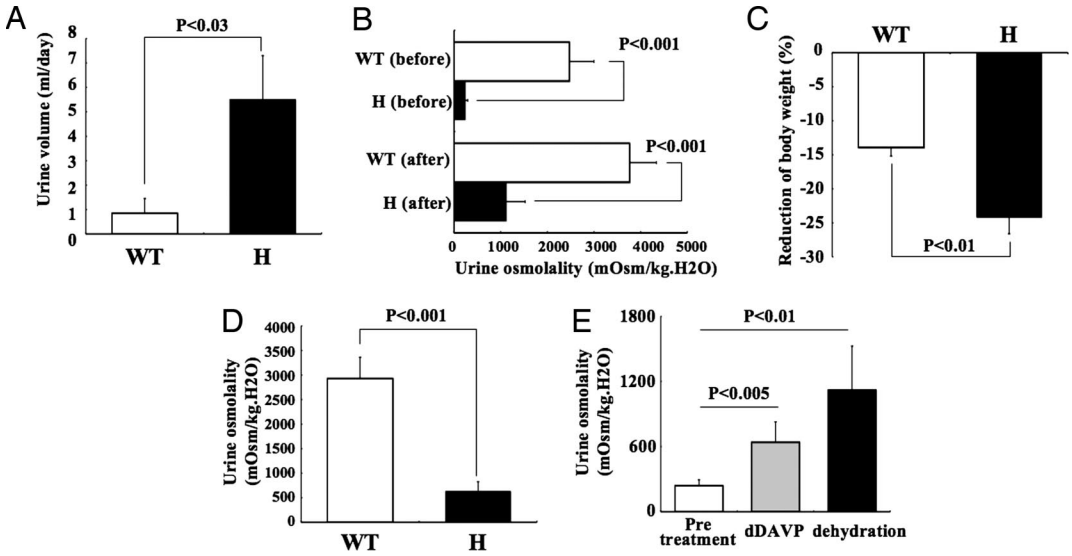

Fig. 2. Urinary-concentrating defect in mutant AQP2 (763–772 del) knockin mice. (*A*) Twenty-four-hour urine volume of wild-type and mutant AQP2 knockin mice. (*B*) Urine osmolality in mice before and after a 24-hr period of water deprivation. (*C*) Reduction of body weight in mice after water deprivation for 24 hr. (*D*) Urine osmolality after i.p. injection of dDAVP (0.4 mg/kg). Mice were injected 60 min before obtaining urine samples. (*E*) Urine osmolality in heterozygous knockin mice before and after dDAVP injection and dehydration for 24 hr. H, heterozygous.

4, $P < 0.001$; Fig. 2*D*). These results indicate impairment of urinary-concentrating ability in heterozygous mutant AQP2 knockin mice. In addition, polyuria-induced hydronephrosis was observed in heterozygous knockin mice (Fig. 3*A*) at 6 wk after birth.

Although heterozygous mutant AQP2 knockin mice exhibited severe impairment of urine-concentrating ability, these mice exhibited partial urine-concentrating ability, which is not observed in the recessive NDI mouse model (10). The heterozygous knockin mice showed significant increases in urine osmolality after dehydration and i.p. injection of dDAVP, respectively (pretreatment, 240 ± 54; dehydration, 1,120 ± 406; dDAVP, 640 ± 188 mOsm/kg H_2O; $n = 4$, P values are shown in Fig. 2*E*).

Sorting Disorder of Mutant AQP2 in Collecting Ducts of Mutant AQP2 Knockin Mice. To investigate the pathogenesis of AD-NDI, we performed immunohistochemistry for AQP2 in collecting duct cells under dehydrated conditions. As shown in Fig. 3*Be*, mutant AQP2 was mainly localized to the basolateral membrane. Mutant AQP2 was predominantly localized to the apical membranes, even under dehydrated conditions. Most wild-type AQP2, which is normally localized at the apical and subapical membranes (Fig. 3*Ba*), was recruited to the basolateral membranes with mutant AQP2, thus demonstrating the *in vivo* dominant-negative effect of mutant AQP2 (Fig. 3*Bd*) on the normal apical targeting of wild-type AQP2. Interestingly, as shown in the merged figure (Fig. 3*Bf*), some targeting of wild AQP2 to the apical membrane was observed, which is consistent with the milder urine-concentrating defect in this mouse model. Double-immunogold staining of collecting duct also confirmed that only the wild-type AQP2 was present in the apical membranes, and that both wild-type and mutant AQP2s were present in basolateral membranes (Fig. 3*C*).

The mechanism of the dominant-negative effect of mutant AQP2 was investigated by verifying the interaction between mutant and wild-type AQP2 *in vivo* using a coimmunoprecipitation assay. As shown in Fig. 3*D*, wild-type AQP2 was coimmunoprecipitated with mutant AQP2 only in the sample from mutant mice. Similarly, mutant AQP2 was coimmunoprecipitated with wild-type AQP2. This evidence indicates that mutant AQP2 binds to wild-type AQP2.

Phosphodiesterase 4 (PDE4) Inhibitor Rolipram Increased Urine Osmolality in Mutant AQP2 Heterozygous Knockin Mice. Phosphorylation of AQP2 by protein kinase A is important for apical targeting (2, 3). Accordingly, intracellular cAMP levels in the collecting ducts are crucial for AQP2 trafficking. In fact, as shown in Fig. 2*E*, dDAVP increased urine osmolality in this mouse model. Here, we investigated whether PDE inhibitors affect urinary concentration ability in heterozygous mutant AQP2 knockin mice. Among the PDE inhibitors tested, rolipram (a PDE4 inhibitor) increased urine osmolality of heterozygous knockin mice, as shown in Fig. 4 (vehicle 295 ± 37 vs. rolipram 783 ± 195 mOsm/kg H_2O, $n = 6$, $P < 0.01$). However, PDE3 (milrinone) and PDE5 inhibitors (sildenafil citrate, Viagra), did not increase urine osmolality, despite the fact that PDE3 and PDE5 are known to be expressed in the collecting ducts (11, 12).

To investigate the mechanism of the action of rolipram, we compared the intracellular localization of AQP2 before and after the administration of rolipram (Fig. 4*B*). Before treatment under a euhydrated condition, wild-type AQP2 was present in cytosol and not concentrated in the apical membranes, as observed in dehydrated mice (Fig. 3*Ba*). Wild-type AQP2 was also present in the basolateral plasma membranes with mutant AQP2. After rolipram treatment, immunofluorescence of wild-type AQP2 in the apical membranes increased, similar to the staining in dehydrated knockin mice (Fig. 3*Bd*). Basolateral localization of mutant AQP2 was unchanged. These findings indicated that rolipram increased the apical translocation of wild-type AQP2 by the same mechanism as AQP2 is regulated by dehydration. In fact, a rolipram-induced increase in urine osmolality was not observed in the dehydrated knockin mice (vehicle 1,195 ± 127 vs. rolipram 1,053 ± 95 mOsm/kg H_2O, $n = 6$), suggesting that dehydration and rolipram share a common signaling pathway. To further confirm this mechanism, we measured cAMP content in the papillae before and after rolipram treatment. As shown in Fig. 4*C*, rolipram increased cAMP content in euhydrated knockin mice, but no further increase was observed in dehydrated knockin mice. The change in cAMP content correlated well with that of urine osmolality. Finally, we observed that rolipram increased the phosphorylation of AQP2 (Fig. 4*D Top*), without affecting the total amount of wild-type AQP2 and mutant AQP2 (Fig. 4*D Bottom*). A similar increase in AQP2 phosphorylation was previously reported to occur shortly

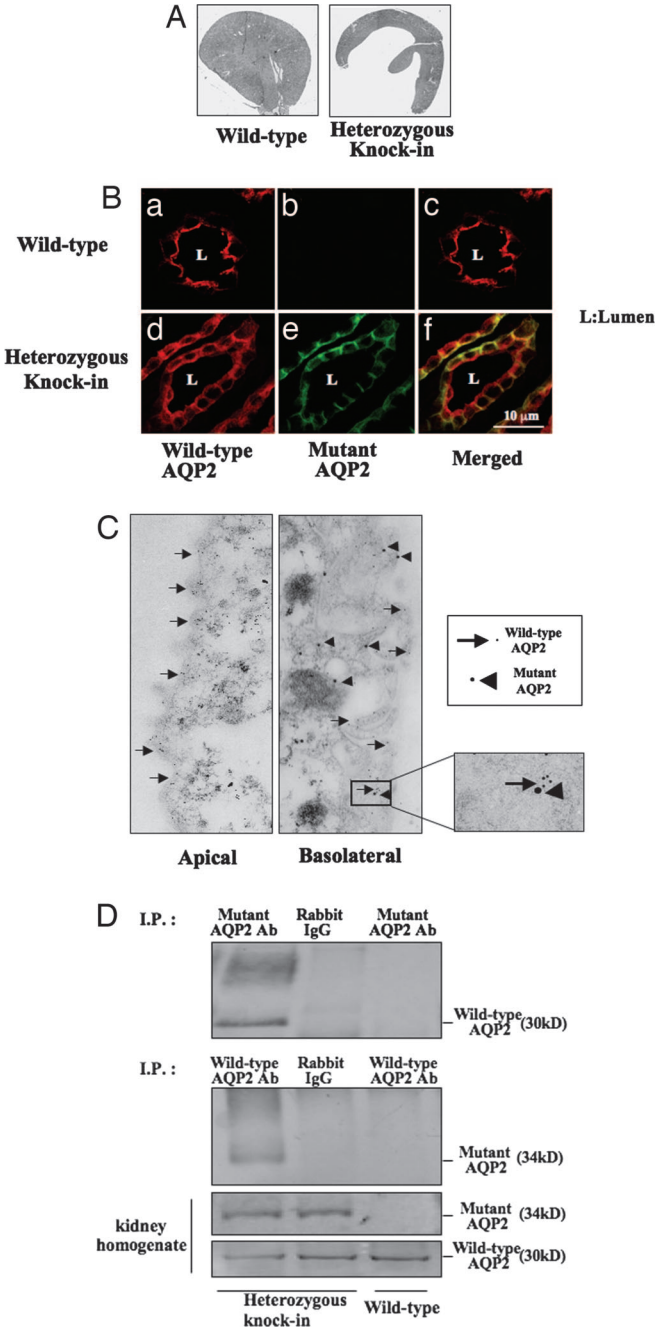

Fig. 3. Renal morphology and localization of wild-type and mutant AQP2 in the collecting duct cells. (*A*) Kidneys from wild-type and mutant AQP2 knockin mice at 8 weeks of age. Polyuria-induced hydronephrosis was observed in mutant mice. (*B*) Double immunofluorescence of wild-type and mutant AQP2 protein in the collecting ducts of wild-type and heterozygous mutant mice. (*a–c*) In wild-type mice, wild-type AQP2 was localized to the apical membrane after dehydration. (*d–f*) Mutant AQP2 was localized to the basolateral membrane. Similarly, wild-type AQP2 is recruited to the basolateral membrane, although some wild-type AQP2 remained in the apical membrane. (*C*) Double-immunogold staining of wild-type and mutant AQP2. Arrows and arrowheads indicate wild-type and mutant AQP2, respectively. Little apical localization of mutant AQP2 and basolateral localization of wild-type AQP2 were seen. (*D*) Coimmunoprecipitation experiments of wild-type and mutant AQP2. Homogenates of kidney papillae from wild-type mouse and heterozygous knockin mouse were immunoprecipitated with mutant AQP2 antibody (*Top*) or wild-type AQP2 antibody (second image from the top). Rabbit IgG was also used as a negative control for immunoprecipitation. Samples immunoprecipitated with wild-type AQP2 were probed with anti-mutant AQP2 antibody and vice versa.

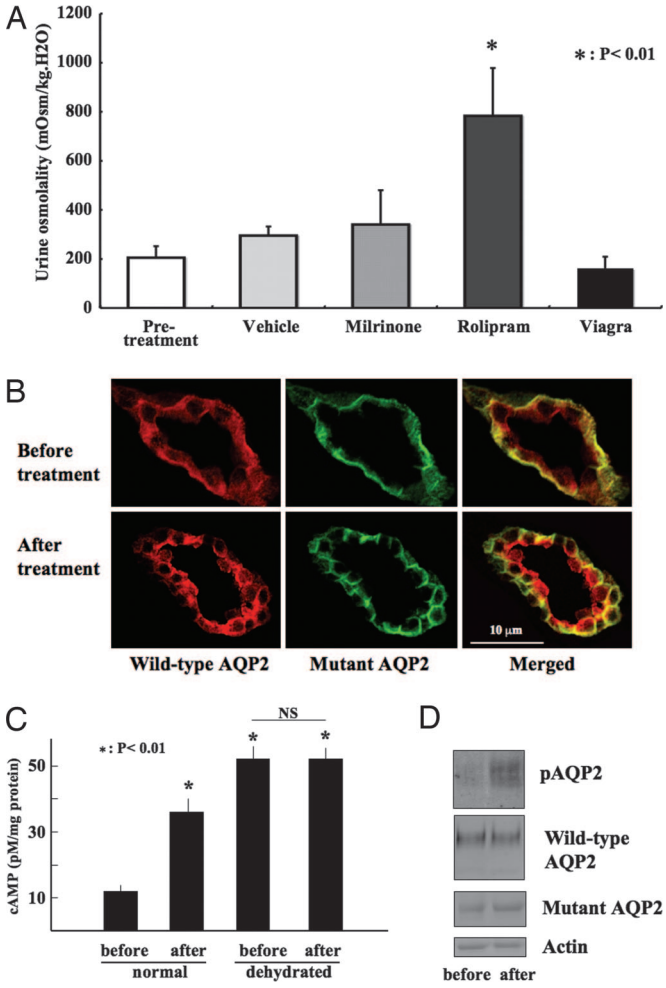

Fig. 4. PDE4 inhibitor increased urine osmolality in mutant AQP2 heterozygous knockin mice. (*A*) Urine osmolality of the heterozygous mutant AQP2 knockin mice before and 1 hr after PDE inhibitor administration. Rolipram, a PDE4 inhibitor, significantly increased urine osmolality in heterozygous knockin mice. (*B*) Immunofluorescence of wild-type and mutant AQP2 before and 1 hr after the administration of rolipram. (C) cAMP content in the papillae before and 1 hr after the administration of rolipram. Rolipram and dehydration increased cAMP content significantly ($P < 0.01$, $n = 4$). However, no further increase in cAMP content was observed by rolipram in dehydrated knockin mice. Dehydration was carried out for 24 hr. (*D*) Western blots of papilla samples from euhydrated knockin mice before and 20 min after the administration of rolipram. The membranes were probed with antibodies against phosphorylated AQP2 (pAQP2), total AQP2, mutant AQP2, and actin.

after dDAVP injection (13). Thus, the signal induced by rolipram was indeed transmitted to AQP2.

Discussion

In this study, we clarified the pathogenesis of dominant-type NDI caused by AQP2 mutation *in vivo* by generating a mutant AQP2 (763–772 del) knockin mouse. In addition, we found that a PDE4 inhibitor, rolipram, was effective in treating this type of NDI.

The mechanisms of AD-NDI caused by mutant AQP2s have only been studied in overexpression systems in either *Xenopus* oocytes or mammalian epithelial cells. Accordingly, it remained unclear whether the dominant-negative effects of mutant AQP2 observed in these overexpression systems was adequate to cause NDI *in vivo*, where mutant AQP2 and wild-type AQP2 expression is driven by each single AQP2 allele. We generated a true mouse model of AD-NDI using gene targeting technology. Even in this model, the

mutant AQP2 level turned out to be less than that of wild-type AQP2 (Fig. 1*G*), possibly because the mutant AQP2 is less stable than the wild-type, or because the remaining single loxP sequence in the mutant allele affects transcription. Nonetheless, the heterozygous mutant AQP2 (763–772 del) knockin mice showed severely impaired urine-concentrating ability (Fig. 2). Furthermore, the mice exhibited milder urine-concentrating defects than T126M mutant AQP2 knockin mice, a mouse model of autosomal-recessive NDI (AR-NDI; ref. 10). T126M mutant mice failed to thrive and generally died by day 6 after birth if they were not artificially given supplemental fluid. Recently generated AQP2 knockout mice also show the same severe urinary-concentrating defect (14). The urine osmolality of T126M mutant mice and AQP2 knockout mice was not increased by dehydration or dDAVP injection. In contrast, AD-NDI model knockin mice survived without supplemental fluid, and urine osmolality increased to some extent after water deprivation or dDAVP injection (Fig. 2*E*). Similar differences in disease severity between recessive and dominant NDI are observed in human NDI. AD-NDI patients are able to increase urine osmolality up to 300–500 mOsm/kg H_2O after water deprivation (6, 7), but AR-NDI patients are rarely able to increase it over 200 mOsm/kg H_2O (15). Thus, the mice generated in this study may provide a good model of human AD-NDI.

Immunofluorescence and immunoelectron microscopy of the collecting ducts explains the milder phenotype of AD-NDI. Mutant AQP2 was mainly localized to the basolateral membranes and was also slightly present in intracellular vesicles. Most of the wild-type AQP2 was recruited to the basolateral membranes with mutant AQP2, but some wild-type AQP2 remained in the apical membranes (Fig. 3*B f* and *i*). Assuming that tetramers containing at least one AQP2 mutant are sorted to the basolateral membrane or remain intracellular, one-sixteenth of all tetramers consist only of wild-type AQP2 and are sorted to the apical membranes. Although apical AQP2 was not quantitatively measured in this study, the above speculation fits with the microscopic findings and milder urine-concentrating defects seen in this mouse model.

At present, a few reports have demonstrated that a mutant protein might cause sorting disorder in the disease like AD-NDI. For example, mutation of a tyrosine motif in the sequence encoding the low-density lipoprotein receptor might result in familial hypercholesterolemia (16). This mutation results in the localization of the receptor to the apical membrane, rather than the basolateral membrane, in Madin–Darby canine kidney (MDCK) cells. AD distal renal tubular acidosis is reported to be caused by a mutation in anion exchanger 1 (AE1) that is usually localized to basolateral membrane (17). This AE1 mutation causes deletion of a tyrosine motif, resulting in aberrant localization to the apical membrane in MDCK cells. Marr *et al.* (18) and Kamsteeg *et al.* (19) analyzed two different types of AQP2 mutations causing AD-NDI. However, all of these sorting disorders have been studied in an overexpression system by using cultured cells. In addition to the problem of overexpression, MDCK cells may not be an ideal system to assess the mechanisms of AQP trafficking, because AQP2 is not endogenously expressed in this cell line. In this respect, this knockin mouse demonstrated the true pathogenesis of AD-NDI and is also an animal model demonstrating that a disease-causing mutant monomer has a dominant-negative effect on the normal sorting of the multimers in *vivo*.

Generation of a mouse model not only confirmed the true mechanism of the disease but also enabled testing of potential therapies. As described above (Fig. 2*E*), dDAVP is able to increase urine osmolality in heterozygous knockin mice. This indicates that the intact wild-type AQP2 that undergoes normal apical translocation by vasopressin signaling is partially preserved in the knockin mice, which is consistent with the immunofluorescence image of wild-type AQP2 in Fig. 3*Bf*. Accordingly, administration of dDAVP is the therapy of choice. However, plasma AVP levels are known to be high in NDI patients because of dehydration (20). Because this leads to down-regulation of the V2 receptor, large amounts of dDAVP are required for actual treatment. Therefore, we focused on PDE as a new therapeutic target. There have been reports of a cAMP-PDE inhibitor improving the activity of the AVP-dependent cAMP system in collecting duct cells in a hypercalcemia-induced NDI mice model (21). In the present study, we found that rolipram, a PDE4 inhibitor, increased urine osmolality in the knockin mice (Fig. 4*A*). Rolipram increased cAMP content in the papillae (Fig. 4*C*), AQP2 phosphorylation (Fig. 4*D*), and AQP2's apical translocation (Fig. 4*B*), all of which were expected based on the known action of this PDE inhibitor. However, which PDE inhibitor was effective for this type of NDI *in vivo* was unknown until this animal model was generated and the drugs actually tested in it. In this study, we tested three PDE inhibitors, including rolipram (Fig. 4*A*). Although PDE3 and PDE5 are thought to be present in the collecting ducts (11, 12), inhibitors of these PDEs were ineffective, thus suggesting that such *in vivo* screening systems are extremely important for testing new therapies and drugs. Recently, F204V AQP2 mutant mice were identified by forward genetic screening (22), while the collecting duct-specific AQP2 knockout mice (14) and inducible AQP2 knockin mice (23) has also been generated. Unlike conventional AQP2 knockin and knockout mice, which die soon after birth, these mouse models, including ours, can survive to adulthood. They should be useful for testing further therapeutic strategies for NDI.

In summary, the present study clearly identifies the pathogenesis of AD-NDI *in vivo*. Genetic diagnosis of congenital NDI is now more important, because this study suggested that AD-NDI is treatable.

Materials and Methods

Generation of Mutant AQP2 (763–772 del) Knockin Mice. Genomic clones containing the AQP2 gene were isolated from a mouse genomic library (Stratagene, La Jolla, CA) by plaque hybridization by using mouse AQP2 cDNA as a probe. Constructs were designed to express the chimeric mutant AQP2 protein whose C terminus was exchanged with that of mutant human AQP2 (763–772 del) using overlap extension PCR (Fig. 1 *A* and *B*). J1 ES cells were electroporated with the targeting construct and selected for resistance to G418 and ganciclovir. To screen for homologous recombinant ES clones, we used PCR with Takara LA *Taq* (Takara Bio, Tokyo, Japan) and the following primers: mouse *aqp2* flanking primer outside of long arm (5′-CATGTACACAGGCAGAG-CAG-3′; F-long arm) and human AQP2-specific primer (5′-CGTCCGTCGGGGCCTTAGAG-3′; R-long arm). This primer set was designed to avoid amplification of the native mouse AQP2 genomic gene. After sequence verification, targeted ES cells were injected into C57BL/6 blastocysts to generate chimeric mice. The resulting male chimeras were mated with female C57BL/6J mice. Tail biopsies from agouti-pigmented F_1 animals were genotyped by PCR of the long arm, as mentioned above (Fig. 1*C*). Additional Southern blot analysis using BglII-digested genomic DNA was used to verify the results of PCR (Fig. 1*D*). To delete the neocassette, the offspring were mated with cytomegalovirus promoter-driven Cre-recombinase transgenic mice. Excision of the neocassette was confirmed by PCR (Fig. 1*E*) by using primers flanking the remaining loxP site (F_1, 5′-AGAATCTACCAGTCCTCAGC-3′; R_1, 5′-CTTGGATACCCAGTCCTTCC-3′). The protocols for these studies were approved by the Institutional Animal Care and Use Committee of Tokyo Medical and Dental University (Certificate of Animal Experimentation, no. 0050119).

Immunoblot Analysis and Immunohistochemistry. We prepared an affinity-purified rabbit antibody raised against the 15 C-terminal amino acids (ASAVSRRGGGCRREP) of the mutant AQP2 (8). For double immunofluorescence, a goat antibody against the C terminus of wild-type AQP2 (Santa Cruz Biotechnology) was used. As shown in Fig. 1*B*, epitopes of the wild-type and mutant AQP2

antibodies were selected to avoid cross-reactions. For immunoblot analysis, kidney tissues were homogenized in a solution containing 0.3 M sucrose, 25 mM imidazole, 1 mM EDTA, and protease inhibitor mixture (Roche Diagnostics, Indianapolis, IN). The tissue homogenate was centrifuged at 4,000 × *g* at 4°C for 15 min twice, and the supernatant was centrifuged 20,000 × *g* at 4°C for 10 min. The resultant pellet was denatured in an SDS sample buffer, separated by SDS/PAGE, and transferred to Hybond-ECL membranes (Amersham, Uppsala, Sweden). Membranes were incubated with primary antibody. Signals were detected by using anti-rabbit or -goat IgG (Fc) alkaline phosphatase conjugate (Promega, Madison, WI) and Western blue (Promega). Deglycosylation of kidney proteins was performed by using an *N*-glycosidase F deglycosylation kit (Roche Diagnostics). To detect phosphorylated AQP2 (pS256), protein samples were prepared in the presence of phosphatase inhibitors (25 mM sodium fluoride/1 mM sodium orthovanadate), and antiphosphorylated AQP2 antibody (a generous gift from S. Nielsen, University of Åarhus, Åarhus, Denmark) was used as the primary antibody. Double-immunofluorescence analysis was performed on cryostat sections of dehydrated mouse kidney by using wild-type and mutant AQP2 antibodies as primary antibodies. Alexa Fluor 488-conjugated donkey anti-rabbit IgG and Alexa Fluor 568-conjugated donkey anti-goat IgG were used as secondary antibodies. Immunofluorescent images were obtained by using an LSM510 laser-scanning confocal microscope system (Zeiss, Jena, Germany).

Double-Immunogold Staining. Sections of dehydrated mouse kidney were incubated with 1% BSA for 30 min at room temperature. After blocking, they were incubated overnight (4°C) with anti-mutant AQP2 antibody. Tissue-bound antibodies were detected by incubating sections with anti-rabbit IgG (H+L) conjugated with 20-nm particles (British Biocell International, London, U.K.). After washing and blocking with BSA, sections were incubated with anti-wild-type AQP2 antibodies overnight at 4°C. Tissue-bound anti-wild-type AQP2 antibodies were detected by using anti-goat IgG (H+L) conjugated with 10-nm gold particles (British Biocell International). Electron microscopic images were obtained by using an electron microscope system (H7000; Hitachi, Tokyo, Japan).

Immunoprecipitation. To prepare protein G Sepharose-linked antibodies, 40 μg of anti-mutant AQP2 antibody, 100 μg of anti-AQP2 antibody, or 100 μg of normal rabbit IgG was mixed with 100 μl of protein G Sepharose 4 fast flow (Amersham). Protein G Sepharose-linked antibodies were washed with 0.15 M sodium borate. Dimethyl pimelimidate was added to cross-link Sepharose and antibody. Cross-linked Sepharose was washed and suspended in PBS with 0.05% sodium azide. Kidney papillae from mice were homogenized in a solution containing 150 mM NaCl, 50 mM Tris·HCl (pH 8.0), and protease inhibitor mixture (Roche Diagnostics). Homogenates were spun at 600 × *g* for 10 min, and 0.5% IGEPAL CA-630 was added to the supernatant. Supernatants were incubated with each protein G Sepharose-linked antibody. Immunoprecipitated samples were analyzed by Western blotting with wild-type or mutant AQP2 antibody.

Animal Study. To investigate urine-concentrating ability, we analyzed 4-wk-old mice. Urine osmolality was measured with a Fiske (Norwood, MA) One-ten Osmometer. In some experiments, mice were injected i.p. with dDAVP (0.4 μg/kg) 60 min before obtaining urine samples. In addition, we used three types of PDE inhibitor to treat the heterozygous mutant AQP2 knockin mice. Rolipram (1 mg/kg) and milrinone (5 mg/kg) dissolved in 20% DMSO were injected i.p. Sildenafil citrate (Viagra, 4 mg/kg) was administered to mice orally. Urine samples were collected before and 1 hr after the administration of each drug. Tissue samples for Western blotting were obtained before and 20 min after treatment.

cAMP Measurement. cAMP content in the papillae was measured by using a cAMP EIA kit (Cayman Chemical, Ann Arbor, MI). Papillae were dissected manually and dispersed in 100 μl of 5% trichloroacetic acid (TCA) by sonication. TCA precipitates were then solubilized in 2 M NaOH and used for measurement of protein content. Supernatants were used for the measurement of cAMP after removing TCA by dimethyl ether extraction.

Statistical Analysis. Results obtained in knockin mice were compared with those in wild-type mice by Student's *t* test. When more than three groups were compared, one-way ANOVA was used followed by Fischer's post hoc test.

We thank J. Miyazaki (Osaka University, Osaka, Japan) for providing the CAG promoter Cre mice; Y. Araki for coimmunoprecipitation; and C. Iijima, M. Goto, and S. Fujii for mouse breeding and genotyping. This study was supported in part by grants-in-aid for Scientific Research on Priority Areas from the Ministry of Education, Culture, Sports, Science and Technology of Japan and by grants-in-aid for Scientific Research on Creative Scientific Research from the Japan Society for the Promotion of Science, the Salt Science Research Foundation, and Astellas Foundation for Research on Metabolic Disorders.

1. Fushimi K, Uchida S, Hara Y, Hirata Y, Marumo F, Sasaki S (1993) *Nature* 361:549–552.
2. Brown D, Katsura T, Gustafson CE (1998) *Am J Physiol* 275:F328–F331.
3. Nielsen S, Chou CL, Marples D, Christensen EI, Kishore BK, Knepper MA (1995) *Proc Natl Acad Sci USA* 92:1013–1017.
4. Yamamoto T, Sasaki S, Fushimi K, Ishibashi K, Yaoita E, Kawasaki K, Marumo F, Kihara I (1995) *Am J Physiol* 268:C1546–C1551.
5. Deen PM, Verdijk MA, Knoers NV, Wieringa B, Monnens LA, van Os CH, van Oost BA (1994) *Science* 264:92–95.
6. Mulders SM, Bichet DG, Rijss JP, Kamsteeg EJ, Arthus MF, Lonergan M, Fujiwara M, Morgan K, Leijendekker R, van der Sluijs P, *et al.* (1998) *J Clin Invest* 102:57–66.
7. Kuwahara M, Iwai K, Ooeda T, Igarashi T, Ogawa E, Katsushima Y, Shinbo I, Uchida S, Terada Y, Arthus MF, *et al.* (2001) *Am J Hum Genet* 69:738–748.
8. Asai T, Kuwahara M, Kurihara H, Sakai T, Terada Y, Marumo F, Sasaki S (2003) *Kidney Int* 64:2–10.
9. Sakai K, Miyazaki, J-I (1997) *Biochem Biophys Res Commun* 237:318–324.
10. Yang B, Gillespie A, Carlson EJ, Epstein CJ, Verkman AS (2001) *J Biol Chem* 276:2775–2779.
11. Bouley R, Pastor-Soler N, Cohen O, McLaughlin M, Breton S, Brown D (2005) *Am J Physiol* 288:F1103–F1112.
12. Homma S, Gapstur SM, Coffey A, Valtin H, Dousa TP (1991) *Am J Physiol* 261:F345–F353.
13. Hoffert JD, Pisitkun T, Wang G, Shen, R-F, Knepper MA (2006) *Proc Natl Acad Sci USA* 103:7159–7164.
14. Rojek A, Fuchtbauer, E-M, Kwon, T-H, Frokiaer J, Nielsen S (2006) *Proc Natl Acad Sci USA* 103:6037–6042.
15. Morello JP, Bichet DG (2001) *Annu Rev Physiol* 63:607–630.
16. Koivisto UM, Hubbard AL, Mellman I (2001) *Cell* 105:575–585.
17. Devonald MA, Smith AN, Poon JP, Ihrke G, Karet FE (2003) *Nat Genet* 33:125–17.
18. Marr N, Bichet DG, Lonergan M, Arthus MF, Jeck N, Seyberth HW, Rosenthal W, van Os CH, Oksche A, Deen PM (2002) *Hum Mol Genet* 11:779–789.
19. Kamsteeg EJ, Bichet DG, Konings IB, Nivet H, Lonergan M, Arthus MF, van Os CH, Deen PM (2003) *J Cell Biol* 163:1099–1109.
20. Zerbe RL, Robertson GL (1981) *N Engl J Med* 305:1539–1546.
21. Wang W, Li C, Kwon TH, Knepper MA, Frokiaer J, Nielsen S (2002) *Am J Physiol* 283:F1313–F1325.
22. Lloyd DJ, Hall FW, Tarantino LM, Gekakis N (2005) *PLoS Genet* 1:171–178.
23. Yang. B., Zhao D, Qian L, Verkman AS (2006) *Am J Physiol* 291: F465–F472.